

## Photoinduced oxygen reordering in $\text{YBa}_2\text{Cu}_3\text{O}_{7-x}$ single crystals

A. G. Panfilov,\* A. I. Rykov, and S. Tajima

*Superconductivity Research Laboratory, International Superconductivity Technology Center, 10-13, Shinonome 1-Chome, Koto-ku, Tokyo 135, Japan*

A. Yamanaka

*Research Institute for Electronic Science, Hokkaido University, Sapporo 060, Japan*

(Received 27 April 1998)

Temporal changes in Raman-scattering spectra of oxygen-deficient  $\text{YBa}_2\text{Cu}_3\text{O}_{7-x}$  single crystals have been studied under exposure of polarized laser light with very low power of the order of  $1 \text{ W/cm}^2$ . Intensities of the additional lines, which appear in Raman spectra because of the imperfectness of oxygen chains, have been found to depend not only on the oxygen content but also on the time elapsed after the beginning of the laser irradiation during Raman measurement. This temporal change obeys the exponential-decay law well with the characteristic time remarkably depending on the temperature. We attribute the observed phenomenon to a metastability of the oxygen ordering in imperfect chains. [S0163-1829(98)04041-7]

### I. INTRODUCTION

It is well known that the illumination of oxygen-deficient ‘‘underdoped’’  $\text{YBa}_2\text{Cu}_3\text{O}_{7-x}$  with visible light has a strong effect on the conduction such as decreasing the normal-state resistivity, inducing the superconductivity in insulating films, or even increasing  $T_c$  by several degrees.<sup>1</sup> To explain these photoinduced effects, several mechanisms have been proposed, among which the charge-transfer and oxygen-diffusion mechanisms are most common. The charge-transfer model suggests the photocreation of electron-hole pairs with the trapping of carriers in the O vacancies.<sup>2</sup> The other one is based on the photoinduced ordering of oxygen atoms, taking into account the relatively high mobility of oxygen in the superconducting oxides.<sup>3</sup> Since the oxygen reordering lowers the average valence of the chain-site copper, transferring holes to the  $\text{CuO}_2$  planes,<sup>4</sup> the two models are interrelated in some sense.

Actually, the local oxygen ordering in imperfect chains is as important as the oxygen content for superconducting properties of the underdoped  $\text{YBa}_2\text{Cu}_3\text{O}_{7-x}$ .<sup>5,6</sup> It is generally believed that the disorder produced by heating is first frozen by the rapid quench, and then the oxygen self-ordering takes place. The self-ordering has been clearly observed at room temperature and exists down to very low temperatures. For example, in  $\text{Tl}_2\text{Ba}_2\text{CuO}_y$ , it can be observed down to 15 K.<sup>7</sup>

As a result of the room-temperature annealing,  $T_c$  in oxygen-deficient crystals increases with time after quenching, reaching an asymptotic value. The complicated sequence of atomic-scale and mesoscale structural transformations leading to different ordered phases has been studied both theoretically and experimentally, showing preferable metastable oxygen distributions at various oxygen contents.<sup>8-11</sup> The rearrangement of the chain oxygens at room temperature has been seen in the modification of Raman-scattering and ellipsometric spectra.<sup>12-14</sup> In spite of the accumulation of a lot of experimental results, the dynamics of the chain oxygen relevant to its ordering has not been clarified yet.

Therefore, the light used for obtaining a Raman spectrum can simultaneously give rise to photoinduced oxygen redistribution (and/or the charge transfer) and thus modify the spectrum. Such a kind of photoinduced effect was observed by Wake *et al.*<sup>15</sup> in the Raman spectrum of the  $\text{YBa}_2\text{Cu}_3\text{O}_7$  crystal. The lines corresponding to nominally forbidden phonon modes lose their intensities under laser irradiation. Therefore, one must keep in mind that in recording a spectrum, there simultaneously occur some spectral changes due to the used light itself.

In the present work, we investigate this photoinduced effect on Raman spectra for various underdoped  $\text{YBa}_2\text{Cu}_3\text{O}_{7-x}$  crystals, aiming at an elucidation of the mechanism of the visible-light action. The effect is pronounced in the additional, so-called ‘‘Raman-forbidden’’ modes, which appear in Raman spectra of oxygen-deficient  $\text{YBa}_2\text{Cu}_3\text{O}_{7-x}$ .<sup>16</sup> As we previously reported,<sup>18</sup> the intensity ratio between the additional  $230 \text{ cm}^{-1}$  line and main  $340 \text{ cm}^{-1}$  one becomes as large as 30 in the  $yy$ -polarized spectrum of  $\text{YBa}_2\text{Cu}_3\text{O}_{7-x}$  with  $T_c = 66 \text{ K}$  at yellow-line laser excitation  $h\nu \sim 2.2 \text{ eV}$ . In this study, we used this striking resonant enhancement of the additional lines to study precisely the time dependence of line intensities and the temperature dependence of the effect.

### II. EXPERIMENT

The Raman-scattering spectra were studied in the pseudo-back-scattering configuration with use of a T64000 Jobin-Yvon triple spectrometer with a liquid-nitrogen cooled charge-coupled detector. The spectral resolution was  $1-3 \text{ cm}^{-1}$ . Lines of Ar-Kr laser were used for the excitation. To avoid nonlinear effects at high incident-laser powers,<sup>19</sup> the power was usually  $2 \text{ W/cm}^2$  on the sample surface ( $5 \text{ mW}$  with a  $0.4 \times 0.8 \text{ mm}^2$  laser spot on a crystal), with local overheating by no more than  $5-10 \text{ K}$ , which was controlled by recording anti-Stokes spectra. The spectra were obtained at  $15 \text{ K}$ , except for the study of temperature dependencies. At low temperatures, a closed-cycle ultrahigh-vacuum cryostat was used with a temperature stability of better than  $1 \text{ K}$ .

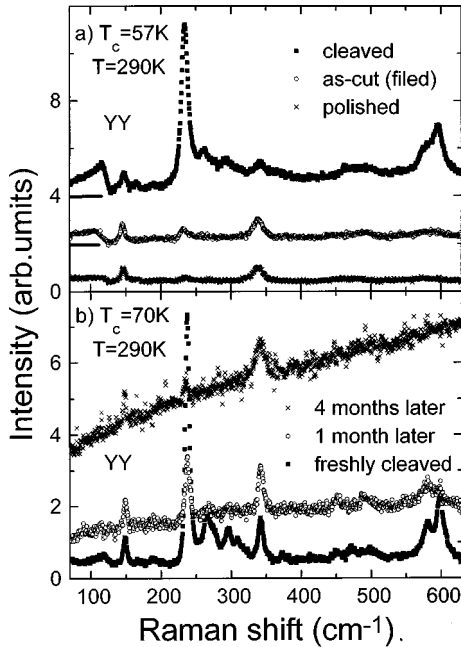


FIG. 1. Degradation and polishing effects on the additional  $230\text{ cm}^{-1}$  line intensity.

Several  $\text{YBa}_2\text{Cu}_3\text{O}_{7-x}$  ( $x=0-0.6$ ,  $T_c=0-93\text{ K}$ ,  $\Delta T_c=2-5\text{ K}$ ) crystals had been prepared and some of them were detwinned as described in Ref. 20. The homogeneity of the samples was carefully checked. The oxygen content was controlled by the annealing temperature for the crystal encapsulated with powder in a quartz tube.<sup>20</sup> The  $7-x$  values were determined by iodometry for the powder or estimated from the lattice parameters determined by the x-ray powder-diffraction measurement.<sup>21</sup> The critical temperatures were determined by a susceptibility measurement in dark conditions. The increase in  $T_c$  due to laser irradiation<sup>3</sup> is expected to be less than 1–2 K in the case of  $T_c > 50\text{ K}$ .

To eliminate the effects of both polishing and crystal degradation, only the freshly cleaved crystal surfaces were studied. Examples of these effects are shown in Fig. 1. The sharp phonon peaks at  $230-300$  and  $560-600\text{ cm}^{-1}$  which are clearly seen for the freshly cleaved surface can noticeably lose their intensities for the polished and as-cut surfaces [Fig. 1(a)]. Similar intensity reduction takes place as a result of the sample degradation accompanied by the increasing luminescence [Fig. 1(b)], which is probably due to the oxygen-atom adsorption on the sample surface.<sup>22</sup>

### III. RESULTS

Figure 2 presents the Raman spectra of a detwinned  $\text{YBa}_2\text{Cu}_3\text{O}_{7-x}$  crystal with  $T_c=70\text{ K}$  in two in-plane polarizations for two laser wavelengths. In addition to the well-known  $B_{1g}$ -like mode at  $340\text{ cm}^{-1}$  and  $A_{1g}$ -like modes at  $115, 150, 440,$  and  $490\text{ cm}^{-1}$ , many additional phonon lines are observed, which are nominally Raman forbidden. Their frequencies are listed in Table I. As reported previously,<sup>15,18</sup> the additional lines showing a resonance at  $2.2\text{ eV}$  are observed only in  $yy$  polarization. (The  $y$  axis is directed along the chains.)

Just after the laser illumination starts, these additional

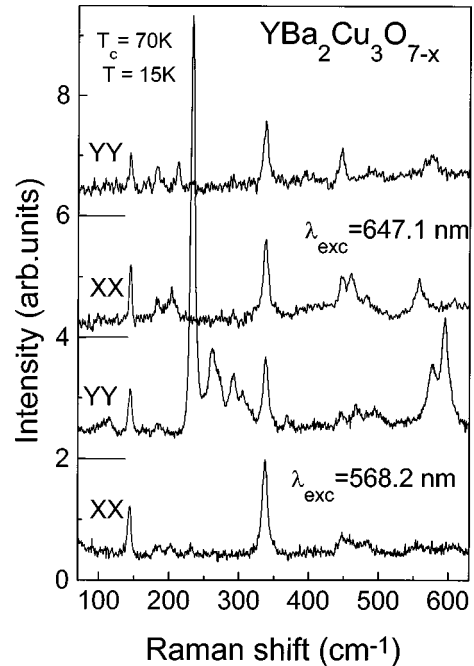


FIG. 2. In-plane polarized Raman spectra of the detwinned  $\text{YBa}_2\text{Cu}_3\text{O}_{7-x}$  single crystal with  $T_c=70\text{ K}$  for two laser-wavelength excitations  $\lambda_{\text{exc}}=568.2$  and  $647.1\text{ nm}$ .  $T=15\text{ K}$ .

lines lose their Raman intensities while the intensity of the main ( $B_{1g}$ - and  $A_{1g}$ -like) lines remains constant. Figure 3 demonstrates the temporal evolution of the  $yy$ -polarized Raman-scattering spectrum for two underdoped  $\text{YBa}_2\text{Cu}_3\text{O}_{7-x}$  with  $T_c=70\text{ K}$  and  $T_c=66\text{ K}$  after the beginning of the laser irradiation with  $\lambda_{\text{exc}}=568\text{ nm}$ . The intensity ratios between the additional lines are constant at the temporal change, indicating that there occurs no intensity redistribution. Note that the lines at about  $230, 260, 290, 360,$  and  $595\text{ cm}^{-1}$  behave in the same manner, showing the same polarization dependence, resonance behavior, and intensity decrease with irradiation.

A similar phenomenon is also observed at different excitation energies. Two examples are shown in Fig. 4 for  $\lambda_{\text{exc}}=488$  and  $647\text{ nm}$ . Though the additional lines are weaker, being out of the resonance at  $2.2\text{ eV}$ , their behavior does not noticeably differ from that at the resonant excitation. Although Wake *et al.*<sup>15</sup> reported that there was no photoinduced effect in oxygenated  $\text{YBa}_2\text{Cu}_3\text{O}_7$  at the illumination with  $h\nu < 2.2\text{ eV}$ , we have found some changes in the spectrum for the red-laser excitation at  $1.9\text{ eV}$  ( $647\text{ nm}$ ).

There are also additional lines of another type, which do not change noticeably under illumination. They are better seen at the red excitation and are observed at different but close wave numbers in  $xx$ - and  $yy$ -polarized spectra (see the upper spectra in Fig. 2 and Table I). We call them  $R_x$  and  $R_y$  lines below. The ‘‘Raman-forbidden’’ lines mentioned above which change their intensities under laser irradiation are called the  $Y_y$  lines hereafter.

In the insets of Figs. 3 and 4, the time dependencies for the  $230\text{ cm}^{-1}$  line intensities are plotted. Owing to practically unchanged line shapes, the intensities could be determined by the intensities at the maxima. The temporal changes were found to obey the exponential-decay law  $I_{230}/I_{340}=A_0 \exp(-t/t_1)+C$  well in every experiment. The

TABLE I. Phonon frequencies ( $\text{cm}^{-1}$ ) at  $T=10$  K. The room-temperature data are given in parentheses (Ref. 23).

YBa <sub>2</sub> Cu <sub>3</sub> O <sub>6</sub>	YBa <sub>2</sub> Cu <sub>3</sub> O <sub>7</sub>	YBa <sub>2</sub> Cu <sub>3</sub> O <sub>6</sub>	YBa <sub>2</sub> Cu <sub>3</sub> O <sub>7</sub>	YBa <sub>2</sub> Cu <sub>3</sub> O <sub>7-x</sub>		
				This work		
Refs. 24, 25, 26	27, 28	24, 24, 25, 26	24, 24, 27, 28	$R_x$	$R_y$	$Y_y$
$E_u$	( $B_{2u}, B_{3u}$ )	$A_{2u}$	$B_{1u}$			
TO (118, 120, 104)	, (102)	104 (104, 108, 114)	113 (103)			121
LO (130, 122, 125)		126 (120, 108, )				
TO			156 (153) 154 (148)	166		168
LO			248 (243)			
TO (193, 189, 211)	181, (185)	145 (145, 156, 147)	194 (194) 191 (216)	185	185	230
LO (207, 198, 206)		216 (215, 187, )	208 (203)			260
TO (250, 248, 247)	240, (239)	214 (213, 216, 188)	275 (283) 281 (353)	203	211	290
LO (270, 265, 266)		227 (223, 225, )	307 (316)			320
TO (357, 355, 354)	345, (340)	366 (364, 370, 426)	312 (314) 311 (430)	460	446	360
LO (409, 416, 417)		474 (468, 466, )	395 (397)			
TO	477,		573 (567) 565 (575)	575	595	575
LO			608 (601)			595
TO (588, 579, 586)	590, (560)	645 (643, 640, )	630 610 (652)	608	640	
LO (617, 629, 645)		669 (667, 661, )				

solid lines in the insets represent the best exponential fitting to the experimental data. As is plotted in Fig. 5, the characteristic decay time  $t_1$  first decreases with temperature and then increases above 200 K.

#### IV. DISCUSSION

##### A. Origin of the additional lines

Prior to our discussion of the mechanism of the photoinduced change in the additional phonon lines, it is necessary to clarify the origin of these lines. The relation of some of the  $Y_y$  lines to the chain oxygen is well known. The 230 and 595  $\text{cm}^{-1}$  lines were ascribed to the vibrations of copper and oxygen in the chains in many reports,<sup>29,30</sup> including the conclusive site-selective oxygen-isotope substitution experiments.<sup>31</sup> Since the additional lines in the spectral region 230–300  $\text{cm}^{-1}$  behave in the same manner [see Fig. 3(b)], all these lines could be related to the chain-oxygen vibrations as well.

For the discussion of the origin of these lines, the following experimental facts should be taken into account. First, as mentioned in Sec. II, the  $Y_y$  line intensities are extremely sensitive to the prehistory of a sample, such as heat treatment, polishing, the aging of a sample in a certain atmosphere, etc. This may indicate that the prehistory affects the chain-oxygen configuration which is responsible for the line appearance. Second, although we do not show the spectrum here, the  $Y_y$  lines diminish in almost-fully oxygenated YBa<sub>2</sub>Cu<sub>3</sub>O<sub>7</sub> with  $T_c=86$  K, which makes it evident that the lines' origin is related to the oxygen deficiency.<sup>32</sup> Third, the  $Y_y$  lines are also absent in heavily oxygen-deficient YBa<sub>2</sub>Cu<sub>3</sub>O<sub>7-x</sub> crystals with  $x>0.6$ . As we found previously,<sup>18</sup> the line intensity is the strongest in YBa<sub>2</sub>Cu<sub>3</sub>O<sub>7-x</sub> with  $x\sim 0.35$  and  $T_c=66\pm 2$  K. For this crystal, the intensity ratio for the 230 and 340  $\text{cm}^{-1}$  lines becomes as large as 30 [see Fig. 3(b)]. For other crystals under study, with higher and lower oxygen content, this ratio was smaller (see Fig. 6). Thus, the line intensity is correlated not

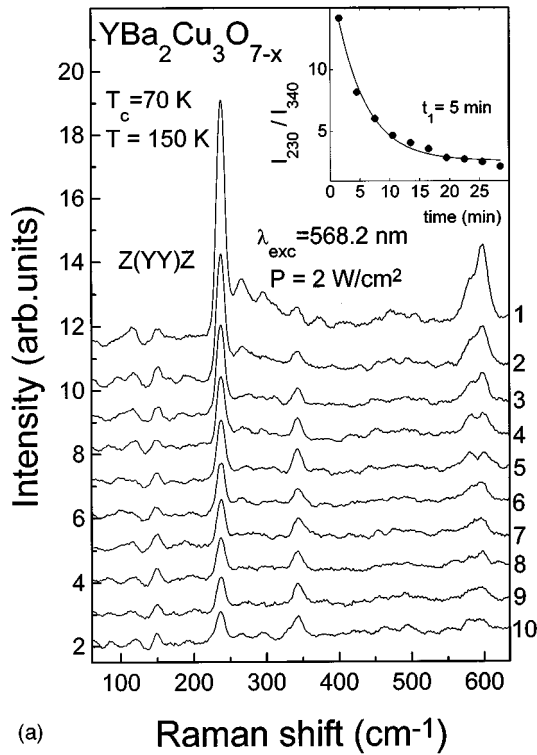
only to the amount of the oxygen deficiency but also to the oxygen occupancy in the chains.

All these facts suggest that the  $Y_y$  lines appear as a result of a particular distribution of oxygens in the chains. Considering the optimum value  $x\sim 0.35$ , the lines are presumably initiated by a special oxygen distribution taking place at  $x=\frac{1}{3}\approx 0.333$  in the so-called ortho-III phase with alternating two full and one empty chains<sup>8,11</sup> or at  $x=\frac{3}{8}=0.375$  in the orthorhombic  $X$  phase with an ordered distribution of oxygen defects.<sup>10,11</sup>

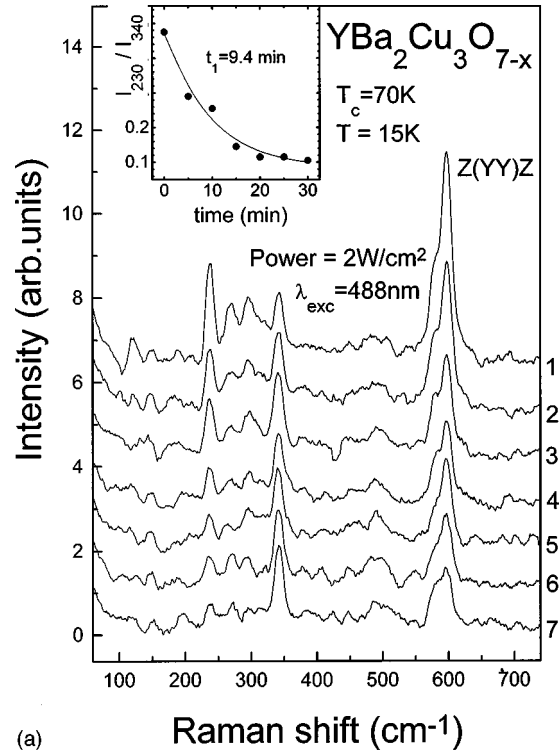
Previously, several explanations have been proposed for the appearance of additional lines in Raman spectra. Such lines could come from microinclusions of dielectric impurity phases.<sup>33</sup> A more reasonable explanation is that the additional lines are a manifestation of the infrared-active phonon branches in the Raman spectra.<sup>29</sup> There can be several mechanisms of such a conversion: (i) an energy resonance of the laser excitation with an electric quadrupole transition,<sup>15</sup> (ii) the Fröhlich electron-phonon interaction in resonant conditions,<sup>26</sup> and (iii) a loss of the site symmetry for atoms participating in the vibration.<sup>30,31</sup>

The first mechanism is unlikely for two reasons. First, the  $yy$ -polarized spectra taken from the ( $ab$ ) and ( $bc$ ) planes of a crystal practically coincide, containing the same sets of lines, and this shows the dipole character of the involved transition. For example, Figs. 3(a) and 4(a) show the  $z(yy)z$  spectra, while the spectra in Figs. 3(b) and 4(b) are taken from the plane containing the  $z$  axis of the twinned crystal with  $T_c=66$  K [ $x(yy)x+y(xx)y$ ]. Second, our measurements showed no threshold energy for the photoinduced effect, which was crucial for the analysis in Ref. 15. Therefore, this conversion mechanism (resonance with an electric quadrupole transition) can be ruled out.

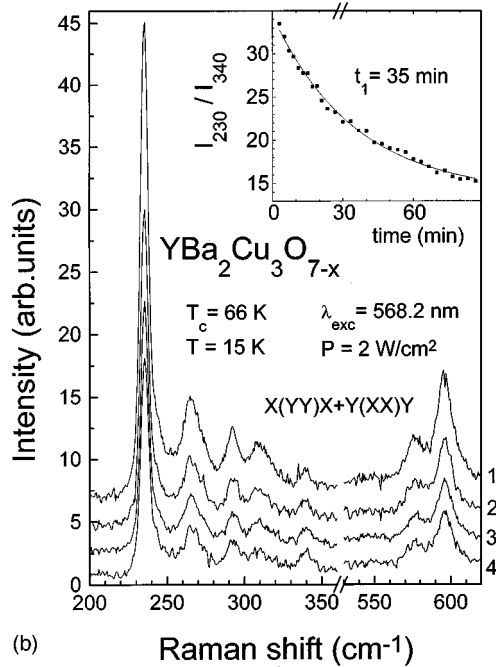
The second mechanism was proposed to explain the additional lines in the insulating YBa<sub>2</sub>Cu<sub>3</sub>O<sub>6</sub>, where the frequencies of these modes and  $LO$  phonons with  $E_u$  symmetry coincide well.<sup>26</sup> For underdoped YBa<sub>2</sub>Cu<sub>3</sub>O<sub>7-x</sub> crystals, there is no agreement between the frequencies of the  $LO$  phonons



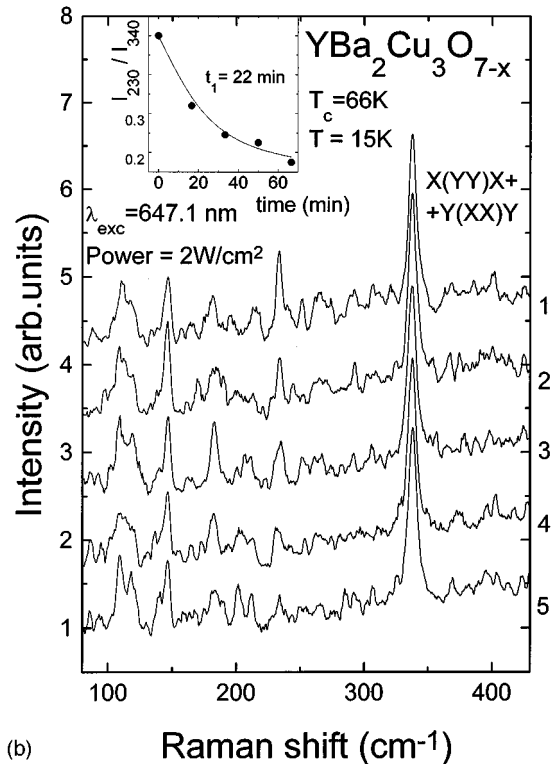
(a)

Raman shift (cm<sup>-1</sup>)

(a)

Raman shift (cm<sup>-1</sup>)

(b)

Raman shift (cm<sup>-1</sup>)

(b)

Raman shift (cm<sup>-1</sup>)

FIG. 3. The temporal changes in the  $yy$ -polarized Raman spectrum of  $\text{YBa}_2\text{Cu}_3\text{O}_{7-x}$  single crystals.  $\lambda_{\text{exc}} = 568.2$  nm. (a)  $T_c = 70$  K,  $T = 150$  K. Spectra 1–10 were taken for 1.5 min each with 1.5 min pauses. (b)  $T_c = 66$  K,  $T = 15$  K. Spectra 1–4 were taken for 1 min each with about 30 min pauses. Insets show the time dependencies of the ratio between the additional  $230$   $\text{cm}^{-1}$  line and the main  $340$   $\text{cm}^{-1}$  one. Solid lines are the best exponential-decay fit  $I_{230}/I_{340} = I_0 \exp(-t/t_1) + I_c$ .

and the  $Y_y$  lines (see Table I). However, the Fröhlich interaction could be considered as a possible reason for the manifestation of the  $R$  lines, especially as these lines are better seen at the red-laser excitation such as the converted originally infrared-active phonons in  $\text{YBa}_2\text{Cu}_3\text{O}_6$ . In Table I, one

FIG. 4. The temporal changes in the  $yy$ -polarized Raman spectrum of  $\text{YBa}_2\text{Cu}_3\text{O}_{7-x}$  single crystals. (a) The same as in Fig. 3(a).  $\lambda_{\text{exc}} = 488$  nm,  $T = 15$  K. Spectra 1–7 were taken for 2.5 min each with 2.5 min pauses. (b) The same as in Fig. 3(b).  $\lambda_{\text{exc}} = 647.1$  nm,  $T = 15$  K. The spectra were taken for 1000 sec each without pauses.

can see that the better frequency correspondence is between the  $B_{2u}(y)$  infrared-active phonons and  $R_x(xx)$  lines, or the  $B_{3u}(x)$  and  $R_y(yy)$  ones, the polarizations given in paren-

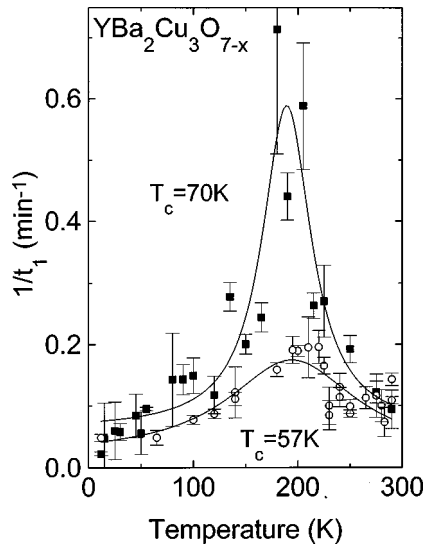


FIG. 5. The temperature dependencies of the inverse characteristic time  $1/t_1$  for two  $\text{YBa}_2\text{Cu}_3\text{O}_{7-x}$  single crystals with  $T_c = 70$  K (filled squares) and  $T_c = 57$  K (open circles). The line is a guide to the eye only.

theses. The phonons from the  $Y_y$ ,  $R_x$ , and  $R_y$  sets can originate from the branches with different symmetries (e.g.,  $B_{1u}$ ,  $B_{2u}$ , and  $B_{3u}$ , correspondingly) and this may explain their different resonant behavior. Thus, although the Fröhlich interaction mechanism could explain appearance of the  $R$  lines and some of the  $Y_y$  ones (at 230 and 595  $\text{cm}^{-1}$ ), the whole set of the  $Y_y$  lines cannot be simply ascribed to the  $\Gamma$ -point odd-parity phonons.

The third mechanism, mode conversion due to the loss of site symmetry, was considered in several variants.<sup>30,31</sup> A deep site-symmetry distortion (for example, when all symmetry elements except for a symmetry plane are lost<sup>30</sup>) leads to the appearance of wide bands in the Raman spectra, reflecting the one-phonon density of states. Such wide bands were actually observed in Ref. 30. In our spectra, however, we can resolve the lines which are narrow enough to exclude the possibility of such a deep site-symmetry distortion. When

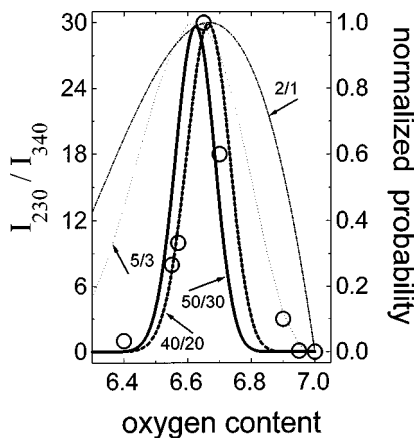


FIG. 6. The oxygen-content dependence of the maximum ratio  $I_{230}/I_{340}$  at  $T = 15$  K (circles) and calculated probabilities of clusters appearing, normalized to the maximum. The probabilities are given for  $m$  oxygens and  $n$  vacancies, where  $m/n$  are 2/1 (dot-dashed line), 5/3 (dotted line), 40/20 (bold dotted line), 50/30 (bold line).

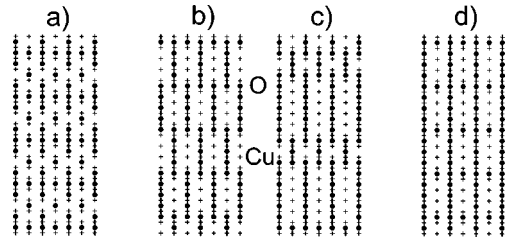


FIG. 7. Possible ordered oxygen distributions for the  $\text{YBa}_2\text{Cu}_3\text{O}_{7-x}$  crystal ( $x = \frac{3}{8}$ ) in the chain plane.

only the inversion is lost,  $\Gamma$ -point odd-parity phonons become Raman active. This case was suggested for atom vibrations at the ends of the chain fragments in underdoped  $\text{YBa}_2\text{Cu}_3\text{O}_{7-x}$  crystals.<sup>31</sup> Based on a molecular model for the finite copper-oxygen chain, Ivanov, Iliev, and Thomsen<sup>31</sup> attributed the 248 and 596  $\text{cm}^{-1}$  bands to the vibrations of, respectively, the copper and oxygen atoms at the end of the chain fragments. Since there are no chain fragments in both  $\text{YBa}_2\text{Cu}_3\text{O}_6$  and  $\text{YBa}_2\text{Cu}_3\text{O}_7$ , this model is consistent with our observation that the  $Y_y$  lines are undetectable in the two parent materials. However, we have observed not a single line but a set of additional lines in the short spectral region around 230–300  $\text{cm}^{-1}$ .

Thus, here we propose another model for the conversion of infrared modes due to oxygen ordering. Let us first consider a simple case of the orthorhombic-II phase  $\text{YBa}_2\text{Cu}_3\text{O}_{6.5}$  with empty and full chains alternating along the  $a$  axis. In this case, the doubling of the unit cell results in the folding of the Brillouin zone. Consequently, the phonon states from the zone boundary, which belong originally to the IR-active  $\Gamma$ -X branches, become the even-parity  $\Gamma$ -point states, which appear in Raman spectra.<sup>34</sup>

In a more general case of the oxygen-deficient  $\text{YBa}_2\text{Cu}_3\text{O}_{7-x}$  crystals, the local ordering is not so simple. In fact there are many orthorhombic phases reported for oxygen-deficient  $\text{YBa}_2\text{Cu}_3\text{O}_{7-x}$ . For example, for  $x = \frac{3}{8}$ , a dozen different theoretically possible orderings have been considered and some of them experimentally found.<sup>8,10,11</sup> Figure 7 illustrates several ordered oxygen distributions in the chain plane for  $x = \frac{3}{8} = 0.375$ . The initial disorder, which was produced by heating and freezing by rapid quenching, disappears owing to the oxygen self-ordering,<sup>8</sup> and a metastable  $X$  phase with the  $2\sqrt{2}a \times 2\sqrt{2}b \times c$  supercell is formed [Fig. 7(a)].<sup>10</sup> As was shown both theoretically<sup>8,35</sup> and experimentally,<sup>12,14,36</sup> further ordering (aging) makes the chain fragments longer, so that the threefold coordinations of oxygens around the chain Cu are converted into twofold and fourfold coordinations. In the limit, a phase which is similar either to the ortho-I or to the ortho-II phase could be formed [Fig. 7(d)] with alternating perfect and nearly empty chains (here, with the occupation number  $\frac{1}{8}$ ). However, other oxygen distributions appear to be thermodynamically preferential, depending also on the procedure of crystal growth and detwinning. Figures 7(b) and 7(c) show two of such possible oxygen distributions.<sup>8</sup>

As a result of the short-range ordering, the Brillouin-zone folding effect makes a few  $\Gamma$ -point phonon states from an infrared-active phonon branch, which can be seen in Raman spectra. The chain-oxygen modes around 200  $\text{cm}^{-1}$  with both the  $B_{2u}$  symmetry and the  $B_{1u}$  have strong dispersion

according to the dynamical calculations<sup>23</sup> and thus could be a source of the additional Raman lines. For example, as a result of the 5/3 ordering [five oxygens and three vacancies in a row, Fig. 7(b)], four additional lines can appear in the Raman spectra, originating from one infrared-active branch. This can explain the appearance of the group of the  $Y_y(yy)$  lines in this spectral region. The folding effect can also give rise to additional electronic  $\Gamma$  states and thus to the resonance at 2.2 eV.

However, a more complicated cluster ordering could be involved, giving a fine structure of the observed lines. Figure 7(c) demonstrates another possible example of the cluster ordering for the composition  $x = \frac{3}{8}$  (a similar pattern was theoretically predicted in the metastable ortho-II phase of the  $\text{YBa}_2\text{Cu}_3\text{O}_{6.5}$  crystal).<sup>8</sup>

Figure 6 shows the calculated oxygen-content dependencies of the appearance probability for the clusters consisting of  $m$  oxygens and  $n$  vacancies, provided that the oxygen distribution is random. The dependencies are normalized to the maximum, which is located at  $x = n/(m+n)$ . For the 5/3 or 2/1 ordering, the maximum is expected to be just at  $7-x = 6.625-6.666$  as is experimentally observed. Comparing the result of these calculations with the experimental results on the intensity ratio  $I_{230}/I_{340}$  (maximum value at  $T = 15$  K), one can find that a cluster consisting of tens atoms/vacancies may be responsible for the manifestation of the  $Y_y$  lines. Since, however, some oxygen distribution can be more preferable thermodynamically, the desired cluster can be smaller.

Summing up, the infrared-Raman conversion of phonons in underdoped  $\text{YBa}_2\text{Cu}_3\text{O}_{7-x}$  crystals can be explained by the short-range ordering of chain oxygen, which gives rise to the folding effects and thus to the manifestation of infrared branches in Raman spectra. Additional support for this model is given by the temporal change of these lines, as discussed below.

### B. The temporal changes in the additional lines

A dramatic decrease in the intensities of the  $Y_y$  lines under the laser irradiation, shown in Figs. 3 and 4, as well as their recovery after switching off the irradiation strongly suggest that these phenomena are governed by the oxygen ordering and/or disordering in the chains. The irradiation moves the oxygen atoms to other empty sites and thus changes the ordering, which can recover after switching the laser off. If it were a mere photoinduced charge transfer, it would affect the intensities of all lines, and shorter characteristic times of the line-intensity decrease and recovery would be observed.

We have found that the temporal changes obey an exponential-decay law  $I_{230}/I_{340} = I_0 \exp(-t/t_1) + I_c$  in every experiment, as is shown in the insets of Figs. 3 and 4. It is worth noting that the residual intensity  $I_c$  was not zero, which reflects the fact that there is no complete destruction of the particular ordering but some clusters with local order exist. Upon switching off the laser, the oxygen atoms which were moved from their initial metastable positions tend to come back. As it is expected, the fewer number of empty sites in the chains that exist, the less time it takes for recovering. In our experiments, at room temperature, this recovery

time varied from a few minutes in optimally doped  $\text{YBa}_2\text{Cu}_3\text{O}_{6.9}$  up to several hours in underdoped  $\text{YBa}_2\text{Cu}_3\text{O}_{7-x}$  crystals with  $x \approx 0.5$ . For the as-grown crystals with  $x \geq 0.6$ , there was no complete restoration of the additional-line intensities. The temperature dependence of the recovery time is of a simple activation type as was found for the  $\text{YBa}_2\text{Cu}_3\text{O}_{6.77}$  sample in Ref. 17.

In contrast to the recovery time, we have found the temperature dependence of the characteristic time  $t_1$  to be quite unusual. With increasing temperature,  $t_1$  first decreases and then shows an upturn above 150–200 K. The peculiarity at about 200 K is clearly seen in Fig. 5, where the temperature dependence of the inverse time  $1/t_1$  is plotted for two crystals. This suggests that the observed temporal changes result from at least two different processes, i.e., the photoinduced reordering and self-ordering. The light illumination disrupts a metastable ordering, presumably making the chain fragments longer [for example, from the distribution shown in Fig. 7(b) to that in Fig. 7(c) and Fig. 7(d) in the limit] and thus decreases the number of clusters which produce additional Raman lines, whereas the self-ordering tends to restore the initial state. Since the probability of the second process also increases with increasing temperature but in a different way, this may slow down the photoinduced changes.

The redistribution, namely, the hopping of oxygen atoms from one metastable position to another over the potential barrier, can be driven by several microscopic mechanisms. First, the local electric fields created by the polarized light can cause the oxygen ions displacement. Second, the energy which is necessary to overcome the barrier can be gained from the phonons created in the scattering processes. Third, the energy can be borrowed from photoexcited carriers. This list of possible mechanisms may not be complete, and further studies are required to distinguish the main reason for the observed phenomena. Considering the oxygen redistribution as the diffusion of the oxygen vacancies, one could apply a diffusion kinetics theory.<sup>37</sup> It predicts different temperature dependencies for the three mechanisms listed above. For example, at low temperatures when self-ordering is not essential, they should give the temperature dependencies of the characteristic time proportional to  $T^{-3/2} \exp(E_0/kT)$ ,  $\exp(E_0/kT)$ , and  $T^{-1/2} \exp(E_0/kT)$ , respectively. However, it is difficult to distinguish one of the mechanisms since the exponential factor dominates. [The Arrhenius plot  $t_1 = t_0 \exp(-E_0/k_B T)$  gives  $E_0$  of the order of a few meV.] At higher temperatures none of the mechanisms alone adequately describes the temperature dependence of  $t_1$ , which indicates the importance of the self-ordering processes. The quantitative analysis is additionally complicated by presumably different preferential metastable order at different temperatures. There is still no general agreement as to the details of the oxygen reordering processes, and further thorough studies on the dependence of the effect on the oxygen content, temperature, and light intensity are thus required.

## V. CONCLUSIONS

Studying the temporal changes in Raman spectra of oxygen-deficient  $\text{YBa}_2\text{Cu}_3\text{O}_{7-x}$  single crystals, we have found that a set of nominally forbidden lines around 230–360  $\text{cm}^{-1}$  and at about 595  $\text{cm}^{-1}$  behaves in the same way

from the viewpoint of dependence on the oxygen content, excitation energy, polarization, and crystal prehistory. A more striking fact is that the intensities of these lines decrease similarly with time under exposure of polarized low-power laser light and recover after switching off the light. The temporal changes obey the exponential-decay law well at any temperature, and the  $T$  dependence of the decay time is not monotonous, with a minimum at about 150–200 K.

None of the models, which have been suggested to explain the nature of the additional lines, can satisfactorily describe all these properties. Therefore, we proposed a refined model for the origin of these additional lines, taking into consideration a particular chain-oxygen ordering. As a result of the ordering, the phonon states from a few points of the Brillouin zone become Raman active.

In this model, the effect of laser irradiation can be interpreted as the oxygen redistribution due to photoinduced hop-

ping of oxygen atoms from the initial metastable positions. Consequently, the intensity recovery after termination of the irradiation is considered as the reordering of a chain-oxygen subsystem to its original state. Several possible microscopic mechanisms for the photoinduced oxygen redistribution were discussed. As for the unusual temperature dependence of the decay time, it must be a result of the balance between processes of disordering and self-ordering, in which the probabilities of both processes increase with increasing temperature but in different manners.

## ACKNOWLEDGMENTS

This work was supported by NEDO for the Research and Development of Industrial Science and Technology Frontier Program.

- \*Permanent address: A. F. Ioffe Physical-Technical Institute, St-Petersburg, Russia.
- <sup>1</sup>J. Hasen, D. Lederman, I. K. Schuller, V. I. Kudinov, M. Maenhoudt, and Y. Bruynseraede, *Phys. Rev. B* **51**, 1342 (1995), and references therein.
  - <sup>2</sup>V. I. Kudinov, I. L. Chaplygin, A. I. Kirilyuk, N. M. Kreines, R. Laiho, E. Lähderanta, and C. Ayache, *Phys. Rev. B* **47**, 9017 (1993).
  - <sup>3</sup>E. Osquiguil, M. Maenhoudt, B. Wuyts, Y. Bruynseraede, D. Lederman, and I. K. Schuller, *Phys. Rev. B* **49**, 3675 (1994).
  - <sup>4</sup>G. Uimin and J. Rossat-Mignod, *Physica C* **199**, 251 (1992).
  - <sup>5</sup>J. D. Jorgensen, Sh. Pei, P. Lightfoot, H. Shi, A. P. Paulikas, and B. W. Veal, *Physica C* **167**, 571 (1990).
  - <sup>6</sup>S. Sadewasser, Y. Wang, J. S. Schilling, H. Zheng, A. P. Paulikas, and B. W. Veal, *Phys. Rev. B* **56**, 14 168 (1997).
  - <sup>7</sup>C. Looney, J. S. Schilling, S. Doyle, and A. M. Hermann, *Physica C* **289**, 203 (1997).
  - <sup>8</sup>S. Semenovskaya and A. G. Khachatryan, *Phys. Rev. B* **46**, 6511 (1992); **54**, 7545 (1983), and references therein.
  - <sup>9</sup>H. Haugerud, G. Uimin, and W. Selke, *Physica C* **275**, 93 (1997), and references therein.
  - <sup>10</sup>M. A. Alario-Franco, C. Chaillout, J. J. Capponi, J. J. Chenavas, and M. Marezio, *Physica C* **156**, 455 (1988).
  - <sup>11</sup>T. Krekels, T. S. Shi, J. Reyes-Gasga, G. van Tendeloo, J. van Landuyt, and S. Amelinckx, *Physica C* **167**, 677 (1990).
  - <sup>12</sup>J. Kircher, E. Brücher, E. Schönherr, R. K. Kremer, and M. Cardona, *Phys. Rev. B* **46**, 588 (1992).
  - <sup>13</sup>V. G. Ivanov, V. G. Hadjiev, and M. N. Iliev, *Physica C* **235-240**, 1255 (1994).
  - <sup>14</sup>A. A. Maksimov, D. A. Pronin, S. V. Zaitsev, I. I. Tartakovskii, G. Blumberg, M. V. Klein, M. Karlow, S. L. Cooper, A. P. Paulikas, and B. W. Veal, *Phys. Rev. B* **54**, R6901 (1996).
  - <sup>15</sup>D. R. Wake, F. Slakey, M. V. Klein, J. P. Rice, and D. M. Ginsberg, *Phys. Rev. Lett.* **67**, 3728 (1991).
  - <sup>16</sup>After our experimental data were obtained we found out about the experiments by Käll *et al.* (Ref. 17). They have extended the investigations by Wake *et al.* (Ref. 15) of the resonance and bleaching effects to the underdoped region.
  - <sup>17</sup>M. Käll, M. Osada, J. Bäckström, M. Kakihana, L. Börjesson, T. Frello, J. Madsen, N. H. Andersen, R. Liang, P. Dosanjh, and W. N. Hardy, *J. Phys. Chem. Solids* (to be published).
  - <sup>18</sup>A. G. Panfilov, M. F. Limonov, A. I. Rykov, S. Tajima, and A. Yamanaka, *Phys. Rev. B* **57**, 5634 (1998).
  - <sup>19</sup>F. Slakey, M. V. Klein, J. P. Rice, and D. M. Ginsberg, *Phys. Rev. B* **42**, 2643 (1990).
  - <sup>20</sup>A. I. Rykov, W.-J. Jang, H. Unoki, and S. Tajima, in *Advances in Superconductivity*, edited by H. Hayakawa and Y. Enomoto (Springer-Verlag, Tokyo, 1996), Vol. VIII, p. 341.
  - <sup>21</sup>Ch. Krüger, K. Conder, H. Schwer, and E. Kaldis, *J. Solid State Chem.* **134**, 356 (1997).
  - <sup>22</sup>I. Ya. Fugol, V. N. Samovarov, Yu. I. Rybalko, and V. M. Zhuravlev, *Mod. Phys. Lett. B* **4**, 803 (1990).
  - <sup>23</sup>One can find more complete information tables on infrared-active phonon frequencies obtained both experimentally and from dynamical calculations in the review by Yu. E. Kitaev, M. F. Limonov, A. P. Mirgorodskii, A. G. Panfilov, and R. A. Evarestov, *Sov. Fiz. Tverd. Tela* **36**, 865 (1994) [*Phys. Solid State* **36**, 475 (1994)].
  - <sup>24</sup>S. Tajima, T. Ido, S. Ishibashi, T. Itoh, H. Eisaki, Y. Mizuo, T. Arima, H. Takagi, and S. Uchida, *Phys. Rev. B* **43**, 10 496 (1991); J. Schützmann, S. Tajima, S. Miyamoto, Y. Sato, and R. Hauff, *ibid.* **52**, 13 665 (1995); S. Tajima and J. Schützmann, *Physica B* **219&220**, 128 (1996).
  - <sup>25</sup>A. V. Bazhenov and V. B. Timofeev, *Supercond. Phys. Chem. Technol.* **3**, 201 (1992).
  - <sup>26</sup>C. Thomsen, M. Cardona, W. Kress, R. Liu, L. Genzel, M. Bauer, E. Schönherr, and U. Schröder, *Solid State Commun.* **65**, 1139 (1988); E. T. Heyen, J. Kircher, and M. Cardona, *Phys. Rev. B* **45**, 3037 (1992).
  - <sup>27</sup>A. V. Bazhenov, *Zh. Eksp. Teor. Fiz.* **102**, 1040 (1992) [*Sov. Phys. JETP* **75**, 566 (1992)].
  - <sup>28</sup>P. Echequt, F. Gervais, K. Dembinsky, M. Gervais, and P. Odier, *Solid State Commun.* **69**, 359 (1989).
  - <sup>29</sup>E. Faulques and V. G. Ivanov, *Phys. Rev. B* **55**, 3974 (1997), and references therein.
  - <sup>30</sup>C. Thomsen, M. Cardona, B. Gegenheimer, R. Liu, and A. Simon, *Phys. Rev. B* **37**, 9860 (1988).
  - <sup>31</sup>V. G. Ivanov, M. Iliev, and C. Thomsen, *Phys. Rev. B* **52**, 13 652 (1995).
  - <sup>32</sup>Our observation appears to contradict the result by Wake *et al.* (Ref. 15) that the resonance and the photoinduced effects on the  $Y_y$  lines can be observed in fully oxygenated  $YBa_2Cu_3O_7$ . However, judging from the spectra in their paper, their crystal seems to be a slightly oxygen-deficient  $YBa_2Cu_3O_{7-x}$  with  $x \approx 0.1$

(which agrees with the reported value of  $T_c=91$  K) rather than a fully oxygenated  $\text{YBa}_2\text{Cu}_3\text{O}_7$  with  $T_c\leq 87$  K. Such spectra also appear as a result of the high incident-laser power of about  $10^2$  W/cm<sup>2</sup>, which could lead to nonlinearly rising “defect oxygen” modes (Ref. 19) presumably because of local structural disordering under laser excitation (Ref. 31).

<sup>33</sup>For example, the line at  $230\text{ cm}^{-1}$  was ascribed by R. Henn, T. Strach, E. Shönher, and M. Cardona, [Phys. Rev. B **55**, 3285 (1997)] to the traces of the  $\text{BaCuO}_2$  phase. However, another line at about  $630\text{ cm}^{-1}$  should dominate in the spectrum of  $\text{BaCuO}_2$  [H. Rosen, E. M. Engler, T. C. Strand, V. Y. Lee, and D. Bethune, *ibid.* **36**, 726 (1987)] and is absent in our spectra. We have found no similarity of the additional-line spectrum

with any impurity-phase one and thus exclude the possibility of impurity-induced modes in our case.

<sup>34</sup>G. E. Blumberg, E. M. Fefer, T. Fimberg, E. Joon, A. Laht, R. Stern, and L. A. Rebane [Solid State Commun. **70**, 647 (1989)] suggested that the additional modes in  $\text{YBa}_2\text{Cu}_3\text{O}_{7-x}$  could be intrinsic Raman-active modes in an ordered ( $2a\times b\times c$ ) supercell.

<sup>35</sup>G. Seder, R. McCormick, and D. de Fontaine, Phys. Rev. B **44**, 2377 (1991).

<sup>36</sup>V. Hadjiev, C. Thomsen, J. Kircher, and M. Cardona, Phys. Rev. B **47**, 9148 (1993).

<sup>37</sup>S. Glasstone, K. J. Laidler, and H. Eyring in *The Theory of Rate Processes*, edited by L. P. Hammett (International Chemical Series, Princeton, 1941).